Buckling of Anisotropic Laminated Cylindrical Plates

James M. Whitney*
Air Force Wright Aeronautical Laboratories, Wright-Patterson Air Force Base, Ohio

An analytical solution is presented for the buckling of anisotropic cylindrical plates under arbitrary combinations of axial load, internal pressure, and in-plane shear load. Donnell-type equations, as applied to laminated cylindrical shells, are used in conjunction with Galerkin's method to determine critical buckling loads. Solutions are obtained and results used to examine the effects of bending-twisting coupling and bending-extensional coupling. Two sets of simply supported boundary conditions are considered.

Introduction

NUMEROUS papers concerning the instability of laminated, anisotropic plates and shells can be found in the open literature. Buckling of layered curved panels has, however, received little attention. Viswanathan et al.[1] obtained solutions for laminated, curved, long rectangular plates subjected to combined loads. Snead and Palazotto[2] studied the effect of moisture absorption and temperature on the buckling of symmetrically laminated cylindrical panels under axial compression. Recently, Zhang and Mathews[3] presented solutions for the buckling of laminated, curved plates under combinations of axial compression and in-plane shear. They formulated the problem in terms of a stress function and transverse displacement. As a result, only force boundary conditions were considered in conjunction with the in-plane portion of the problem. Analysis of laminated curved plates is of current interest because of the potential use of composite materials in fuselage and wing structure.

In the current paper a buckling analysis of laminated, anisotropic cylindrical plates under arbitrary combinations of axial load, internal pressure, and in-plane shear loading is presented. Emphasis is placed on in-plane shear and axial load. Donnell-type equations as applied to laminated shells[4] are utilized in conjunction with Galerkin's method[5] to obtain critical buckling loads. Effects of bending-twisting coupling and bending-extensional coupling are examined.

For many engineering applications of curved plates, the ratio of in-plane dimensions to thickness will be greater than 50:1. In such cases shear deformation will not be significant for practical engineering laminate.[6,7] Thus, in the current paper, shear deformation is not considered. In addition, ratios of radius of curvature to plate thickness are often in excess of 500:1. Hence, Donnell's theory should provide sufficient accuracy.[8]

Although buckling analysis in conjunction with Donnell's theory has traditionally been formulated in terms of a stress function and transverse displacement, Galerkin's method provides a straightforward approach utilizing displacements. Since the method is based on variational principles, proper boundary conditions are clearly defined. In addition, such an approach is very appropriate for problems involving in-plane displacement boundary conditions. Although the complete displacement formulation adds one more equation compared to the stress function, transverse displacement approach, it poses little additional numerical difficulty. It should also be noted that a complete displacement formulation has often been utilized in conjunction with unsymmetrically laminated plates.[9]

Presented as Paper 83-0979 at the AIAA/ASME/ASCE/AHS 24th Structures, Structural Dynamics, and Materials Conference, Lake Tahoe, Nevada, May 2-4, 1983; received May 1, 1983; revision submitted Dec. 3, 1983. This paper is declared a work of the U.S. Government and therefore is in the public domain.

*Materials Research Engineer, Nonmetallic Materials Division, Materials Laboratory. Associate Fellow AIAA.

Governing Equations

A standard Cartesian coordinate system is located at the center of the plate, as illustrated in Fig. 1. The plate thickness, radius of curvature, and in-plane dimensions are denoted by h, R, a, and b, respectively. In addition, the plate is composed of an arbitrary number of layers with arbitrary fiber orientation in each layer. The midplane displacements in the x, s, and z directions are denoted by u^0, v^0, and w, respectively.

Strain-Displacement Relations

The Donnell-type equations[4] are based on the following normalized strain-displacement relations, with a comma denoting partial differentiation:

$$\epsilon_\zeta = \epsilon_\zeta^0 + \bar{z}\kappa_\zeta, \quad \epsilon_\eta = \epsilon_\eta^0 + \bar{z}\kappa_\eta, \quad \epsilon_{\zeta\eta} = \epsilon_{\zeta\eta}^0 + \bar{z}\kappa_{\zeta\eta} \tag{1}$$

where

$$\epsilon_\zeta^0 = U_{,\zeta}; \quad \epsilon_\eta^0 = AV_{,\eta} + SW; \quad \epsilon_{\zeta\eta}^0 = V_{,\zeta} + AU_{,\eta}$$

$$\kappa_\zeta = -W_{,\zeta\zeta}; \quad \kappa_\eta = -A^2 W_{,\eta\eta}; \quad \kappa_{\zeta\eta} = -2AW_{,\zeta\eta} \tag{2}$$

and

$$U = u^0/h; \quad V = v^0/h; \quad W = w/a$$

$$A = a/b; \quad S = a^2/Rh; \quad \zeta = x/a; \quad \eta = s/b; \quad \bar{z} = z/h$$

with midplane strains and curvatures denoted by ϵ^0 and κ, respectively.

Constitutive Relations

The strain-displacment relations, Eqs. (1) and (2), combined with force and moment resultants, lead to the following normalized plate constitutive relations

$$\begin{bmatrix} N_\zeta \\ N_\eta \\ N_{\zeta\eta} \\ M_\zeta \\ M_\eta \\ M_{\zeta\eta} \end{bmatrix} = \begin{bmatrix} a_{11} & a_{12} & a_{16} & b_{11} & b_{12} & b_{16} \\ a_{12} & a_{22} & a_{26} & b_{12} & b_{22} & b_{26} \\ a_{16} & a_{26} & a_{66} & b_{16} & b_{26} & b_{66} \\ b_{11} & b_{12} & b_{16} & d_{11} & d_{12} & d_{16} \\ b_{12} & b_{22} & b_{26} & d_{12} & d_{22} & d_{26} \\ b_{16} & b_{26} & b_{66} & d_{16} & d_{26} & d_{66} \end{bmatrix} \begin{bmatrix} \epsilon_\zeta^0 \\ \epsilon_\eta^0 \\ \epsilon_{\zeta\eta}^0 \\ \kappa_\zeta \\ \kappa_\eta \\ \kappa_{\zeta\eta} \end{bmatrix} \tag{3}$$

Denoting in-plane ply stresses by σ_i, then

$$(N_i, M_i) = \frac{a}{hE_T} \int_{-1/2}^{1/2} \sigma_i(1, \bar{z})\, d\bar{z}$$

and

$$(a_{ij}, b_{ij}, d_{ij}) = \frac{1}{E_T} \int_{-1/2}^{1/2} Q_{ij}(1, \bar{z}, \bar{z}^2)\, d\bar{z}$$

where Q_{ij} are the anisotropic reduced stiffnesses for plane stress. The normalizing modulus, E_T, represents the transverse modulus (direction perpendicular to the fibers) of a unidirectional ply. For a hybrid laminate E_T represents the transverse modulus of one of the ply materials.

Governing Equations in Operator Form

The governing equations in nondimensional form are as follows:

$$\begin{aligned} L_{11}U + L_{12}V + L_{13}W &= 0 \\ L_{12}U + L_{22}V + L_{23}W &= 0 \\ L_{13}U + L_{23}V + L_{33}W &= \bar{N}_\zeta W_{,\zeta\zeta} + 2A\bar{N}_{\zeta\eta} W_{,x\zeta} + A^2 \bar{N}_\eta W_{,\eta\eta} \end{aligned} \tag{4}$$

Denoting prebuckled average axial and shear stresses through the thickness by $\bar{\sigma}_\zeta$ and $\bar{\sigma}_{\zeta\eta}$, respectively, then

$$\bar{N}_\zeta = \frac{\bar{\sigma}_\zeta}{E_T}\left(\frac{a}{h}\right)^2; \quad \bar{N}_{\zeta\eta} = \bar{\sigma}_{\zeta\eta}\left(\frac{a}{h}\right)^2; \quad \bar{N}_\eta = \frac{Ra^2 p}{E_T h^3} \tag{5}$$

and p is the internal pressure. The L_{ij} are linear operators defined as follows:

$$\begin{aligned} L_{11} &= a_{11}(\,)_{,\zeta\zeta} + 2a_{16}A(\,)_{,\zeta\eta} + a_{66}A^2(\,)_{,\eta\eta} \\ L_{12} &= a_{16}(\,)_{,\zeta\zeta} + (a_{12}+a_{66})A(\,)_{,\zeta\eta} + a_{26}A^2(\,)_{,\eta\eta} \\ L_{13} &= a_{12}S(\,)_{,\zeta} + a_{26}SA(\,)_{,\eta} - b_{11}(\,)_{,\zeta\zeta\zeta} \\ &\quad - 3b_{16}A(\,)_{,\zeta\zeta\eta} - (b_{12}+2b_{66})A^2(\,)_{,\zeta\eta\eta} - b_{26}A^3(\,)_{,\eta\eta\eta} \\ L_{22} &= a_{66}(\,)_{,\zeta\zeta} + 2a_{26}A(\,)_{,\zeta\eta} + a_{22}A^2(\,)_{,\eta\eta} \\ L_{23} &= a_{26}S(\,)_{,\zeta} + a_{22}SA(\,)_{,\eta} - b_{16}(\,)_{,\zeta\zeta\zeta} \\ &\quad - (b_{12}+2b_{66})A(\,)_{,\zeta\zeta\eta} - 3b_{26}A^2(\,)_{,\zeta\eta\eta} - b_{22}A^3(\,)_{,\eta\eta\eta} \\ L_{33} &= d_{11}(\,)_{,\zeta\zeta\zeta\zeta} + 4D_{16}A(\,)_{,\zeta\zeta\zeta\eta} + 2(d_{12}+2d_{66})A^2(\,)_{,\zeta\zeta\eta\eta} \\ &\quad + 4d_{16}A^3(\,)_{,\zeta\eta\eta\eta} + d_{22}A^4(\,)_{,\eta\eta\eta\eta} \\ &\quad - b_{12}S(\,)_{,\zeta\zeta} - 4b_{26}SA(\,)_{,\zeta\eta} - 2b_{22}SA^2(\,)_{,\eta\eta} + a_{22}S^2(\,) \end{aligned} \tag{6}$$

Galerkin Method

Two sets of simple support boundary conditions are considered in the present paper. The first set is referred to as BC-1.

At $\zeta = 0, 1$:

$$N_\zeta = M_\zeta = V = W = 0 \tag{7}$$

At $\eta = 0, 1$:

$$N_\eta = M_\eta = U = W = 0 \tag{8}$$

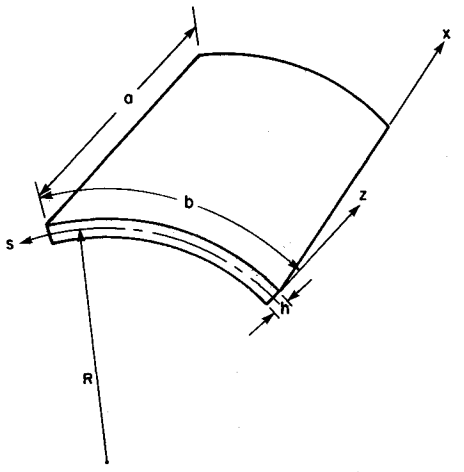

Fig. 1 Nomenclature for curved laminated plate.

The second set of boundary conditions, denoted BC-2, represents fully clamped in-plane boundary conditions.

At $\zeta = 0, 1$:

$$U = V = W = M_\zeta = 0 \tag{9}$$

At $\eta = 0, 1$:

$$U = V = W = M_\eta = 0 \tag{10}$$

A solution to the problem is sought in the form

$$\begin{aligned} U &= \sum_{m=1}^{\infty}\sum_{n=1}^{\infty} A_{mn}\phi_{mn}(\zeta,\eta) \\ V &= \sum_{m=1}^{\infty}\sum_{n=1}^{\infty} B_{mn}\chi_{mn}(\zeta,\eta) \\ W &= \sum_{m=1}^{\infty}\sum_{n=1}^{\infty} C_{mn}\psi_{mn}(\zeta,\eta) \end{aligned} \tag{11}$$

The functions ϕ_{mn}, χ_{mn}, and ψ_{mn} must satisfy the displacement boundary conditions. The Galerkin method[5] leads to the following equations for BC-1.

$$\int_0^1\int_0^1 (L_{11}U + L_{12}V + L_{13}W)\phi_{mn}\, d\zeta d\eta + \int_0^1 [N_\zeta(0,\eta)\phi_{mn}(0,\eta) - N_\zeta(1,\eta)\phi_{mn}(1,\eta)]d\eta = 0 \tag{12}$$

$$\int_0^1\int_0^1 (L_{12}U + L_{22}V + L_{23}W)\chi_{mn}\, d\zeta d\eta + \int_0^1 [N_\eta(\zeta,0)\chi_{mn}(\zeta,0) - N_\eta(\zeta,1)\chi_{mn}(\zeta,1)]d\zeta = 0 \tag{13}$$

$$\begin{aligned} &\int_0^1\int_0^1 (L_{13}U + L_{23}V + L_{33}W - \bar{N}_\zeta W_{,\zeta\zeta} - 2A\bar{N}_{\zeta\eta}W_{,\zeta\eta} \\ &\quad - A^2\bar{N}_\eta W_{,\eta\eta})\psi_{mn}\, d\zeta d\eta + \int_0^1 [M_\zeta(0,\eta)\psi_{mn,\zeta}(0,\eta) \\ &\quad - M_\zeta(1,\eta)\psi_{mn,}(1,\eta)]d\eta + \int_0^1 [M_\eta(\zeta,0)\psi_{mn,\eta}(\zeta,0) \\ &\quad - M_\eta(\eta,1)\psi_{mn,\eta}(\zeta,1)]d\zeta = 0 \end{aligned} \tag{14}$$

Table 1 Convergence of Galerkin method

Shear buckling $[+45_3/-45_3]_s$
graphite-epoxy, Eq. (18), $a/b=1$, $S=90$

M	N	$\|\lambda\|$ (<0)	$\|\lambda\|$ (>0)
		BC-1	
2	2	475.590	518.36
4	4	105.640	208.45
6	6	92.271	207.25
8	8	91.395	207.18
10	10	91.035	207.16
		BC-2	
2	2	1830.60	1873.30
4	4	202.69	328.09
6	6	112.65	282.48
8	8	109.68	279.85
10	10	108.94	279.11

Equations (12-14) yield a set of linear algebraic equations in the form of a classic eigenvalue problem from which critical buckling loads can be determined. For boundary conditions BC-2, Eqs. (12-14) are valid except the integrals involving N_ζ and N_η will vanish exactly, due to the fully clamped in-plane boundary conditions.

The following functions will be utilized in conjunction with BC-1:

$$\phi_{mn}=\cos m\pi\zeta\sin n\pi\eta,\quad \chi_{mn}=\sin m\pi\zeta\cos n\pi\eta$$

$$\psi_{mn}=\sin m\pi\zeta\sin n\pi\eta \tag{15}$$

These functions will satisfy all of the displacement boundary conditions, but not necessarily the natural boundary conditions. The line integrals in Eqs. (12-14) are a consequence of not satisfying the natural boundary conditions. For BC-2 the first two equations in (15) are replaced by the functions

$$\phi_{mn}=\chi_{mn}=\sin m\pi\zeta\sin n\pi\eta \tag{16}$$

and all of the displacement boundary conditions are exactly satisfied.

Some special cases in conjunction with BC-1 are of particular interest. If all of the shear coupling terms vanish ($a_{16}=a_{26}=b_{16}=b_{26}=d_{16}=d_{26}=0$), then Eqs. (11) and (15) lead to an exact solution to Eqs. (4), which satisfy all of the required boundary conditions, Eqs. (7) and (8), for arbitrary combinations of axial load and internal pressure. For cases where $a_{16}=a_{26}=b_{16}=b_{26}=0$, Eqs. (15) will lead to an exact solution for the first two equations in Eq. (4) with the natural boundary conditions $N_\zeta(0,\eta)=N_\zeta(1,\eta)=N_\eta(\zeta,0)=N_\xi(\zeta,1)=0$ being exactly satisfied. These equations can then be solved for A_{mn} and B_{mn} in terms of C_{mn}. The results are then substituted into Eq. (14). Thus, for this case only one of the three Galerkin equations need be utilized.

For the general case, Eqs. (12) and (13) are solved for A_{mn} and B_{mn} in terms of C_{mn} and substituted into Eq. (14). If the infinite series is truncated at $m=M$ and $n=N$, then Eq. (14) produces an $M\times N$ set of equations in classical eigenvalue form. The resulting equations can be divided into two groups, one correponding to $m+n$ even and one corresponding to $m+n$ odd.

Numerical Results

Consider two 12-layer angle-ply laminates with the stacking geometries $[+45_3/-45_3]_s$ and $[(\pm45)_3]_s$ under pure in-plane shear loading. The first stacking geometry behaves as a 4-ply laminate. This allows two stacking sequences of the same class of laminate geometry (i.e., the $[\pm45]_s$ class of laminates), to be investigated without changing laminate thickness. Since the laminate is symmetric, $b_{ij}=0$. The in-plane properties are orthotropic ($a_{16}=a_{26}=0$), while the bending stiffnesses are anisotropic. For the class of laminates $[(\pm45°)_N]_s$, the bending-twisting coupling terms are of the form

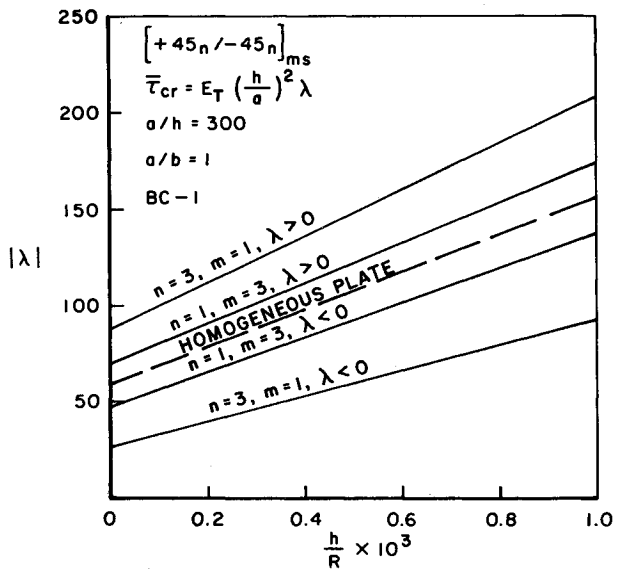

Fig. 2 Shear buckling of symmetric angle-ply, graphite-epoxy curved plates.

$$d_{16}=d_{26}=\frac{Q_{16}(45°)}{16E_TN} \tag{17}$$

where N is the number of repeating units of $\pm45°$ layers above the midplane. Thus, the effect of bending-twisting coupling terms will dissipate with an increasing number of units of $\pm45°$ layers. Numerical results are presented in Table 1 and Fig. 2 for a laminate with the following ply properties:

$$E_L/E_T=14,\ G_{LT}/E_T=0.5,\ \nu_{LT}=0.25 \tag{18}$$

These are typical properties of current graphite-epoxy composite materials. A 12-ply graphite-epoxy plate is approximately 1.52 mm (0.06 in.) thick. Thus, an 457×457 mm (18×18 in.) panel would result in $a/h=300$, and

$$s=(a/h)^2(h/R)=90{,}000(h/R)$$

Convergence of the solution is shown in Table 1, while the effect of plate curvature is illustrated in Fig. 2. Note that bending-twisting coupling effects increase with increasing curvature. This is especially noticeable in the case of the four-layer composite. The presence of bending-twisting coupling results in different critical buckling loads for positive and negative shear.

Results for unsymmetric laminates under pure shear of the class $[\pm45]_N$ are shown in Fig. 3. In order to maintain a 12-ply thickness, the two stacking geometries considered are $[+45_6/-45_6]$ and $[+45_3/-45_3]_2$. The first geometry corresponds to a two-ply laminate and the second to a four-ply laminate. For this class of laminates both the in-plane and bending properties were orthotropic ($a_{16}=a_{26}=d_{16}=d_{26}=0$), while the only nonvanishing bending-extensional coupling terms are b_{16} and b_{26}, which are of the form

$$b_{16}=b_{26}=Q_{16}(45°)/4E_TN \tag{19}$$

where N is the total number of repeating ±45 units. Note that the difference between critical loads for positive and negative shear are small, but do depend on plate curvature. For flat plates positive and negative shear yield identical critical loads.

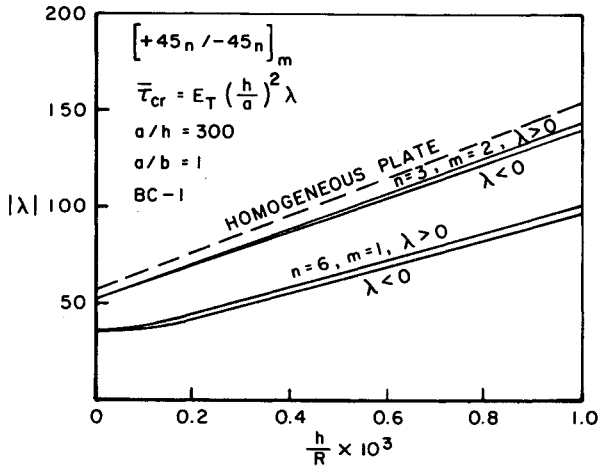

Fig. 3 Shear buckling of unsymmetric angle-ply, graphite-epoxy curved plates.

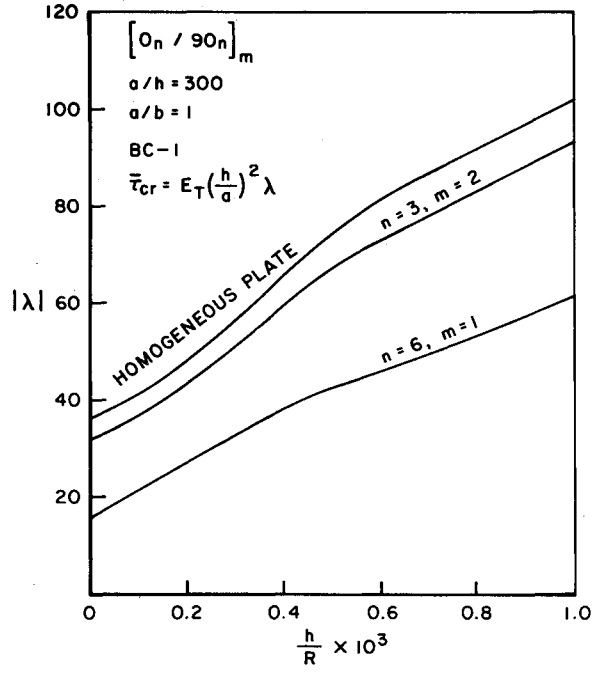

Fig. 4 Shear buckling of unsymmetric cross-ply, graphite-epoxy curved plates.

The effect of twisting-extensional coupling is seen to dissipate rapidly with increasing $\pm 45°$ ply units.

Now consider two 12-layer unsymmetric cross-ply laminates with the stacking geometries $[0_6/90_6]$ and $[0_3/90_3]_2$ under in-plane shear loading. The first stacking geometry behaves as a two-ply laminate and the second as a four-ply laminate. This again allows two stacking sequences of the same class of laminate (i.e., the [0/90] unsymmetric class of laminates) to be studied without changing laminate thickness. For this class of laminate $a_{16}=a_{26}=b_{16}=b_{26}=d_{16}=d_{26}=0$. The only bending-extensional coupling terms that do not vanish are b_{11} and b_{22}. For the class of unsymmetric laminates $[0/90]_N$, the bending-extensional coupling terms are of the form

$$b_{22} = -b_{11} = (1/8E_TN)[Q_{11}(0°) - Q_{22}(0°)] \qquad (20)$$

where N is the total number of repeating units of 0°/90° layers. Numerical results are presented in Fig. 4 for the ply

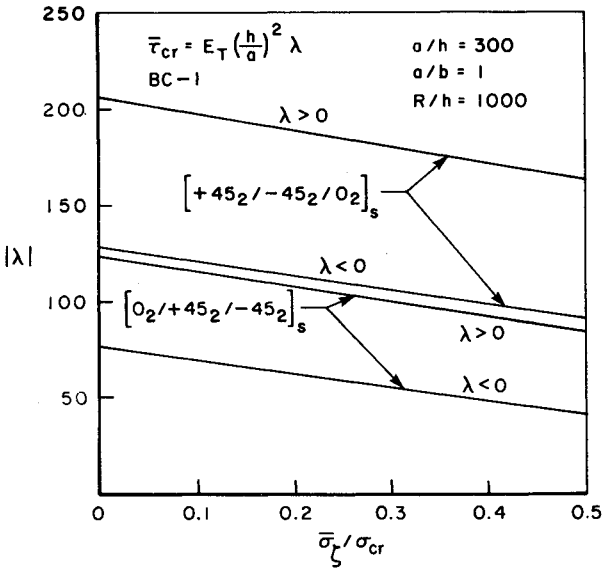

Fig. 5 Shear buckling under combined axial compression and in-plane shear for symmetric angle-ply, graphite-epoxy curved plates.

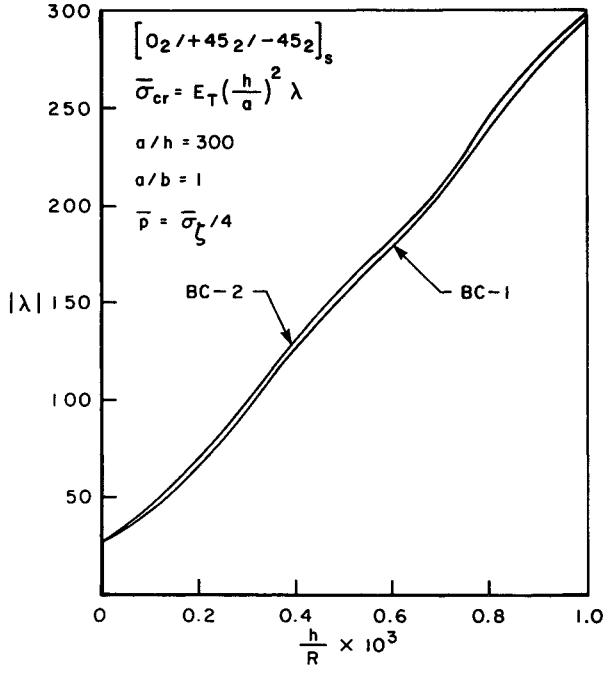

Fig. 6 Comparison of boundary conditions for compression buckling of angle-ply, graphite-epoxy curved plates under axial compression and internal pressure.

properties given in Eq. (18). Again the effect of bending-extensional coupling is seen to dissipate rapidly with an increasing number of layers.

Note that the homogeneous solutions in Figs. 2-4 are obtained by allowing $N \to \infty$ in Eqs. (17), (19), and (20).

The effect of stacking sequence geometry on combined axial compression and torsion is shown in Fig. 5 for symmetric laminates of the class $[0/\pm 45]_s$. Ply properties are those of Eq. (18). Critical shear buckling loads are shown for increasing axial compression loads. The axial loads are normalized by the critical buckling load, σ_{cr}, associated with the same laminate under uniaxial compression. As one might anticipate, the laminate with angle-plies on the outer surfaces produces greater shear stability. It also produces the largest

difference in critical buckling load between positive and negative shear.

The effect of in-plane boundary conditions on critical buckling load for laminates under combined axial compression and internal pressure is shown in Fig. 6, where $\bar{p}$ is the normalized internal pressure denoted by p/E_T. Laminate geometry is of the same class as considered in Fig. 5, and the ply properties are those of Eq. (18). As can be easily seen, the two boundary conditions under consideration produce very little difference in critical buckling load.

Conclusions

The Galerkin method provides an efficient approach to the buckling analysis of laminated, anisotropic curved panels. Such analytical methods are a viable alternative approach to the finite element method.

Numerical results indicate that the effects of anisotropy and bending-extensional coupling on critical buckling loads can be influenced by plate curvature.

References

[1] Viswanathan, A. V., Tamekuni, M., and Baker, L. L., "Elastic Stability of Laminated, Flat and Curved Long Rectangular Plates Subjected to Combined and Plain Loads," NASA CR-2330, June 1974.

[2] Snead, J. M. and Palazotto, A. N., "Moisture and Temperature Effects on the Instability of Cylindrical Composite Panels," AIAA Paper 82-0741, *Proceedings of the AIAA/ASME/AHS/ASCE 23rd Structures, Structural Dynamics and Materials Conference*, Pt. 1, New York, 1982, pp. 279-286.

[3] Zhang, Y. and Mathews, F. L., "Initial Buckling of Curved Panels of Generally Layered Composite Materials," *Composite Structures*, Vol. 1, June 1983, pp. 3-30.

[4] Dong, S. B., Pister, K. S., and Taylor, R. L., "On the Theory of Laminated Anisotropic Shells and Plates," *Journal of the Aerospace Sciences*, Vol. 29, Sept. 1962, pp. 969-975.

[5] Kantorovich, L. V. and Krylov, V. I., *Approximate Methods of Higher Analysis*, translated by C. D. Benster, Interscience, New York, 1958.

[6] Whitney, J. M. and Pagano, N. J., "Shear Deformation in Heterogeneous Anisotropic Plates," *Journal of Applied Mechanics*, Vol. 37, Dec. 1970, pp. 1031-1036.

[7] Whitney, J. M and Sun, C. T., "A Refined Theory for Laminated Anisotropic Cylindrical Shells," *Journal of Applied Mechanics*, Vol. 41, June 1974, pp. 471-476.

[8] Pagano, N. J. and Whitney, J. M., "Geometric Design of Composite Cylindrical Characterization Specimens," *Journal of Composite Materials*, Vol. 4, July 1970, pp. 360-378.

[9] Ashton, J. E. and Whitney, J. M., *Theory of Laminated Plates*, Technomic Publishing Co., Stamford, Conn., 1970.